DMD Fast Forward. Published on November 8, 2012 as DOI: 10.1124/dmd.112.049460
DMD Fast Forward. Published on November 8, 2012 as doi: 10.1124/dmd.112.049460
This article has not been copyedited and formatted. The final version may differ from this version.

Title of the article:

Analysis of the repaglinide concentration increase produced by gemfibrozil and itraconazole based on the inhibition of the hepatic uptake transporter and metabolic enzymes

Names of authors:

Toshiyuki Kudo, Akihiro Hisaka, Yuichi Sugiyama, Kiyomi Ito

Affiliations:

Research Institute of Pharmaceutical Sciences, Musashino University, 1-1-20 Shinmachi, Nishitokyo-shi, Tokyo 202-8585, Japan (T.K., K.I.)

Pharmacology and Pharmacokinetics, University of Tokyo Hospital, 7-3-1 Hongo, Bunkyo-ku, Tokyo 113-8655, Japan (A.H.)

RIKEN Innovation Center, RIKEN, Research Cluster for Innovation, RIKEN (The Institute of Physical and Chemical Research), RIKEN Yokohama Bio Industry Center 2F, 1-6 Suehiro-cho, Tsurumi-ku, Yokohama 230-0045, Japan (Y.S.)

Downloaded from dmd.aspetjournals.org at ASPET Journals on April 19, 2024

Copyright 2012 by the American Society for Pharmacology and Experimental Therapeutics.

DMD Fast Forward. Published on November 8, 2012 as DOI: 10.1124/dmd.112.049460
This article has not been copyedited and formatted. The final version may differ from this version.

Running Title: PBPK analysis of repaglinide DDI with OATP/CYP inhibitors

Address correspondence:

Kiyomi Ito, Ph.D.

Musashino University

Research Institute of Pharmaceutical Sciences

1-1-20 Shinmachi, Nishitokyo-shi, Tokyo 202-8585, Japan

Tel/Fax: +81-42-468-9199

E-mail: k-ito@musashino-u.ac.jp

Number of text pages: 40

Number of figures: 4

Number of tables: 3

Number of references: 52

Number of words in the Abstract: 238

Number of words in the Introduction: 869

Number of words in the Discussion: 947

Abbreviations:

Downloaded from dmd.aspetjournals.org at ASPET Journals on April 19, 2024

DMD Fast Forward. Published on November 8, 2012 as DOI: 10.1124/dmd.112.049460
This article has not been copyedited and formatted. The final version may differ from this version.

AUC, area under the concentration-time curve; β, CL_{int} divided by (CL_{int} + PS_{eff}); C_b, concentrations in the blood compartment; C_e, concentration in the liver extracellular space compartment; C_h, concentrations in the liver compartment; CL_h, hepatic clearance; CL_{int}, intrinsic metabolic clearance; $CL_{int,all}$, overall intrinsic clearance; $CL_{int,h}$, hepatic intrinsic clearance; CL_{NH}, non-hepatic clearance; cLogP, logarithm of the computer-calculated partition coefficient between n-octanol and water; CL_{tot}, total body clearance; CYP, cytochrome P450; F_a, fraction absorbed; f_b, blood unbound fraction; f_e, urinary excretion ratio of parent drug; F_g, intestinal availability; F_h, hepatic availability; f_h, unbound fraction in the liver; fm_{2C8}, fraction metabolized by CYP2C8; GEM, gemfibrozil; GEM-glu, gemfibrozil glucuronide; IC_{50}, half maximal inhibitory concentration; ICZ, itraconazole; k_{12}, transfer rate constant from the blood compartment to the peripheral compartment; k_{21}, transfer rate constant from the peripheral compartment to the blood compartment; k_a, absorption rate constant; $k_{deg,2C8}$, the first-order rate constant for degradation of CYP2C8; $K_{i,1B1}$, inhibition constant for hepatic uptake; $K_{i,3A4}$, the inhibition constant for CYP3A4-mediated hepatic metabolism; $k_{i,app,2C8}$, the apparent inhibition constant for CYP2C8-mediated hepatic metabolism; $k_{inact,2C8}$, the maximum inactivation rate constant for CYP2C8-mediated hepatic metabolism; K_p, liver-to-plasma concentration ratio; Lag, lag time for

Downloaded from dmd.aspetjournals.org at ASPET Journals on April 19, 2024

DMD Fast Forward. Published on November 8, 2012 as DOI: 10.1124/dmd.112.049460
This article has not been copyedited and formatted. The final version may differ from this version.

absorption; OATP, organic anion transporting polypeptide; PBPK, physiologically based pharmacokinetic; PK, pharmacokinetic; PS_{eff}, intrinsic clearance for the efflux from hepatocytes to blood; PS_{inf}, intrinsic clearance for hepatic uptake from blood; Q_h, hepatic blood flow; R2C8, inhibition ratio of CYP2C8; R3A4, inhibition ratio of CYP3A4; R_b, blood-to-plasma concentration ratio; Rinf, inhibition ratio of hepatic uptake; V_b, distribution volume in the blood compartment; V_e, volume of the liver extracellular space; V_h, volume of liver; X_{sub}, amount in the peripheral compartment

Downloaded from dmd.aspetjournals.org at ASPET Journals on April 19, 2024

DMD Fast Forward. Published on November 8, 2012 as DOI: 10.1124/dmd.112.049460
This article has not been copyedited and formatted. The final version may differ from this version.

Abstract

The plasma concentration of repaglinide is reported to increase greatly when given after repeated oral administration of itraconazole and gemfibrozil. The present study analyzed this interaction based on a physiologically based pharmacokinetic (PBPK) model incorporating inhibition of the hepatic uptake transporter and metabolic enzymes involved in repaglinide disposition. Firstly, the plasma concentration profiles of inhibitors (itraconazole, gemfibrozil and gemfibrozil glucuronide) were reproduced by a PBPK model to obtain their pharmacokinetic parameters. The plasma concentration profiles of repaglinide were then analyzed by a PBPK model, together with those of the inhibitors, assuming a competitive inhibition of CYP3A4 by itraconazole, mechanism-based inhibition of CYP2C8 by gemfibrozil glucuronide, and inhibition of OATP1B1 by gemfibrozil and its glucuronide. The plasma concentration profiles of repaglinide were well reproduced by the PBPK model based on the above assumptions and the optimized values for the inhibition constants (0.0676 nM for itraconazole against CYP3A4; 14.2 μM for gemfibrozil against OATP1B1; and 5.48 μM for gemfibrozil glucuronide against OATP1B1) as well as the fraction of repaglinide metabolized by CYP2C8 (0.801) were consistent with the reported values. The validity of the obtained parameters was further confirmed by sensitivity analyses and by

Downloaded from dmd.aspetjournals.org at ASPET Journals on April 19, 2024

DMD Fast Forward. Published on November 8, 2012 as DOI: 10.1124/dmd.112.049460
This article has not been copyedited and formatted. The final version may differ from this version.

reproducing the repaglinide concentration increase produced by concomitant gemfibrozil administration at various timings/doses. The present findings suggested that the reported concentration increase of repaglinide, suggestive of synergistic effects of the co-administered inhibitors, can be quantitatively explained by the simultaneous inhibition of the multiple clearance pathways of repaglinide.

Downloaded from dmd.aspetjournals.org at ASPET Journals on April 19, 2024

DMD Fast Forward. Published on November 8, 2012 as DOI: 10.1124/dmd.112.049460
This article has not been copyedited and formatted. The final version may differ from this version.

Introduction

Repaglinide is one of the short-acting meglitinide analogues that reduce blood glucose concentrations by enhancing glucose-stimulated insulin secretion from pancreatic beta cells (Fuhlendorff et al., 1998). It has been reported that the plasma concentration of repaglinide after an oral dose was dramatically increased when it was given following repeated oral administration of itraconazole (ICZ; 100 mg) and gemfibrozil (GEM; 600 mg) twice a day for 3 days in healthy volunteers (the AUC of repaglinide was increased 1.4-, 8.1- and 19.4-fold by ICZ, GEM, and both, respectively) (Niemi et al., 2003a). The major route of repaglinide elimination from the body is active uptake from blood into hepatocytes by an uptake transporter, organic anion transporting polypeptide (OATP) 1B1, followed by biotransformation by cytochrome P450 (CYP) enzymes (CYP3A4 and CYP2C8) into several metabolites (van Heiningen et al., 1999; Bidstrup et al., 2003; Kajosaari et al., 2005a; Niemi et al., 2005; Kalliokoski et al., 2008). Therefore, the above interactions possibly resulted from inhibitions of OATP1B1, CYP3A4 and CYP2C8.

The plasma repaglinide concentration after oral administration in humans has been reported to be affected by genetic polymorphisms of OATP1B1 and CYP2C8: for OATP1B1, subjects with the 521CC genotype have a significantly higher (1.7- to

Downloaded from dmd.aspetjournals.org at ASPET Journals on April 19, 2024

DMD Fast Forward. Published on November 8, 2012 as DOI: 10.1124/dmd.112.049460
This article has not been copyedited and formatted. The final version may differ from this version.

2.9-fold) repaglinide AUC than those with the wild-type (521TT) (Niemi et al., 2005; Kalliokoski et al., 2008); for CYP2C8, subjects with the CYP2C8*1/*3 genotype have a significantly lower (0.5-fold) repaglinide AUC than those with wild-type (*1/*1) (Niemi et al., 2003b; Niemi et al., 2005). On the other hand, there was no difference in the AUC of repaglinide between the subjects with the CYP3A4 *1/*18 genotype and those with the wild-type (*1/*1) (Ruzilawati and Gan, 2010).

The co-administered inhibitors of OATP1B1, CYP2C8 and CYP3A4 have also been reported to affect the disposition of repaglinide: the AUC of oral repaglinide was significantly increased by co-administration of clarithromycin (1.4-fold) (Niemi et al., 2001) and cyclosporine (2.4-fold) (Kajosaari et al., 2005b) which are known to inhibit both OATP1B1 and CYP3A4; co-administration of telithromycin and trimethoprim, an inhibitor of CYP3A4 and CYP2C8, respectively, increased the AUC of oral repaglinide by 1.8-fold (Kajosaari et al., 2006) and 1.6-fold (Niemi et al., 2004), respectively. It has also been reported that repeated administration of rifampicin, an inducer of CYP enzymes including CYP3A4 and CYP2C8, significantly reduced the AUC of oral repaglinide (0.2- or 0.4-fold) (Niemi et al., 2000; Bidstrup et al., 2004).

ICZ is known to be a potent reversible inhibitor of CYP3A4. In in vitro studies using human liver microsomes, ICZ strongly inhibited the biotransformation of

Downloaded from dmd.aspetjournals.org at ASPET Journals on April 19, 2024

DMD Fast Forward. Published on November 8, 2012 as DOI: 10.1124/dmd.112.049460
This article has not been copyedited and formatted. The final version may differ from this version.

substrates of CYP3A4, such as midazolam, quinidine and testosterone (von Moltke et al., 1996; Galetin et al., 2005). The AUCs of oral triazolam and midazolam, both eliminated from the body mainly by CYP3A4-mediated metabolism, were significantly increased when co-administered with ICZ (200 mg, p.o., o.d., for 4 days) by 27- and 6.2-fold, respectively (Varhe et al., 1994; Backman et al., 1998).

GEM inhibited the CYP2C8-mediated metabolism of paclitaxel and cerivastatin in human liver microsomes without affecting the CYP3A4-mediated hydroxylation of testosterone (Wang et al., 2002; Shitara et al., 2004). It was also found that GEM glucuronide (GEM-glu) is a mechanism-based inhibitor of CYP2C8 (Ogilvie et al., 2006), and this was supported by a persistent interaction between GEM and repaglinide in vivo (Tornio et al., 2008). Both GEM and GEM-glu are also reported to inhibit OATP1B1 in in vitro studies using human hepatocytes and OATP1B1-expressing cells (Shitara et al., 2004; Nakagomi-Hagihara et al., 2007). The AUCs of oral pravastatin and rosuvastatin, mainly taken up into the liver by OATP1B1 and excreted into bile in unchanged forms, were significantly increased when co-administrated with GEM (600 mg, p.o., b.i.d., for 3 days) by 2- and 1.9-fold, respectively (Kyrklund et al., 2003; Schneck et al., 2004). In addition, the AUC of cerivastatin, a substrate of OATP1B1 and CYP2C8, was significantly increased when co-administered with GEM (600 mg, p.o.,

Downloaded from dmd.aspetjournals.org at ASPET Journals on April 19, 2024

DMD Fast Forward. Published on November 8, 2012 as DOI: 10.1124/dmd.112.049460
This article has not been copyedited and formatted. The final version may differ from this version.

b.i.d., for 3 days) by 4.4-fold (Backman et al., 2002), and this was suggested to result from the inhibition of OATP1B1 and CYP2C8 by both GEM and GEM-glu (Shitara et al., 2004).

Taken together, these pieces of evidence supports the hypothesis that the reported drastic increase in the AUC of repaglinide resulted from the inhibition of OATP1B1, CYP3A4 and CYP2C8 by ICZ or GEM. The present study aimed to analyze this interaction quantitatively using a physiologically based pharmacokinetic (PBPK) model for all the compounds (repaglinide, GEM and GEM-glu) involved in the interaction. Although PBPK models have been used for the quantitative prediction of the degree of drug-drug interaction involving metabolic enzymes (Kanamitsu et al., 2000; Ito et al., 2003; Kato et al., 2008; Zhang et al., 2009; Rowland-Yeo et al., 2010; Zhao et al., 2012), and also for describing the disposition of a drug transporter substrate pravastatin (Watanabe et al., 2009), only ‘static’ approaches have been used for the interactions at drug transporters (Hinton et al., 2008; Yoshida et al., 2012), with no reports on the application of PBPK modeling to the best of our knowledge. In the present study, we investigated whether the increase in repaglinide AUC by ICZ and GEM can be quantitatively explained based on the clearance concept and a PBPK model incorporating the inhibition of both the hepatic uptake transporter and metabolic

Downloaded from dmd.aspetjournals.org at ASPET Journals on April 19, 2024

DMD Fast Forward. Published on November 8, 2012 as DOI: 10.1124/dmd.112.049460
This article has not been copyedited and formatted. The final version may differ from this version.

enzymes.

Downloaded from dmd.aspetjournals.org at ASPET Journals on April 19, 2024

DMD Fast Forward. Published on November 8, 2012 as DOI: 10.1124/dmd.112.049460
This article has not been copyedited and formatted. The final version may differ from this version.

Materials and Methods

1. Calculation of pharmacokinetic parameters for repaglinide

The urinary excretion of repaglinide is reported to be negligible (0.1%) after its intravenous administration to healthy volunteers (van Heiningen et al., 1999). Therefore, the total body clearance (CL_{tot}) was assumed to be equal to the hepatic clearance (CL_h) and the hepatic availability (F_h) was calculated as $1 - CL_h/Q_h$, where Q_h represents the hepatic blood flow (86.9 L/hr) (Watanabe et al., 2009). As the bioavailability (0.625) estimated from an oral/intravenous administration study (Hatorp, 2002) exceeds the estimated F_h of 0.40 (0.25-0.52 using the Q_h of 70-110 L/hr), a product of F_a and F_g, where F_a and F_g represent the fraction absorbed and the intestinal availability, respectively, was assumed to be unity. Thus, the overall intrinsic clearance ($CL_{int,all}$) for hepatic elimination of repaglinide, multiplied by the blood unbound fraction (f_b), was calculated by the following equation using the AUC values reported in the interaction study with ICZ/GEM (4.74, 6.66, 38.3, and 91.5 ng hr/mL for control, +ICZ, +GEM, and +ICZ+GEM, respectively) (Niemi et al., 2003a).

$$f_b \cdot CL_{int,all} = \frac{Dose}{AUC} \qquad \text{(Eq. 1)}$$

where Dose is the oral dose of repaglinide (0.25 mg for all conditions).

Downloaded from dmd.aspetjournals.org at ASPET Journals on April 19, 2024

DMD Fast Forward. Published on November 8, 2012 as DOI: 10.1124/dmd.112.049460
This article has not been copyedited and formatted. The final version may differ from this version.

2. Estimation of the inhibition ratio of intrinsic clearances for each process based on the AUC increase produced by ICZ and GEM

The $CL_{int,all}$ calculated above is expressed as follows (Shitara et al., 2006):

$$CL_{\mathrm{int},all} = \frac{PS_{\mathrm{inf}} \cdot CL_{\mathrm{int}}}{CL_{\mathrm{int}} + PS_{eff}} = \frac{PS_{\mathrm{inf}} \cdot CL_{\mathrm{int}} / PS_{eff}}{CL_{\mathrm{int}} / PS_{eff} + 1} = \frac{PS_{\mathrm{inf}} \cdot \gamma}{1+\gamma} = PS_{\mathrm{inf}} \cdot \beta \qquad \text{(Eq. 2)}$$

where PS_{inf} and PS_{eff} represent the intrinsic clearance for hepatic uptake from blood and the efflux from hepatocytes to blood, respectively; γ is defined as CL_{int}/PS_{eff}; β, defined as $CL_{int}/(CL_{int}+PS_{eff})$, can be used for evaluating the rate-limiting process of hepatic intrinsic clearance. CL_{int} represents the intrinsic clearance for hepatic metabolism mediated by CYP2C8 and CYP3A4, which can be expressed as follows using the fraction metabolized by CYP2C8 (fm_{2C8}):

$$CL_{\mathrm{int}} = CL_{int\,2C8} + CL_{int\,3A4} = fm_{2C8} \times CL_{int} + (1 - fm_{2C8}) CL_{int} \qquad \text{(Eq. 3)}$$

For the control (administration of repaglinide alone), the following equations can be derived from the above equations:

$$\boldsymbol{AUC_{cont}} = \frac{\boldsymbol{Dose_{cont}}}{\boldsymbol{f_b \cdot PS_{\mathrm{inf}} \times \frac{\gamma}{1+\gamma}}} \qquad \text{(Eq. 4)}$$

Assuming that ICZ inhibits CYP3A4, the following equations can be derived for +ICZ (co-administration of ICZ) condition:

Downloaded from dmd.aspetjournals.org at ASPET Journals on April 19, 2024

DMD Fast Forward. Published on November 8, 2012 as DOI: 10.1124/dmd.112.049460
This article has not been copyedited and formatted. The final version may differ from this version.

$$AUC_{+ICZ} = \frac{Dose_{+ICZ}}{fb \cdot PS_{inf} \times \frac{\gamma_{+ICZ}}{1+\gamma_{+ICZ}}} \quad \text{(Eq. 5)}$$

$$\gamma_{+ICZ} = fm_{2C8} \times \gamma + (1 - fm_{2C8}) \times \gamma \times R3A4 \quad \text{(Eq. 6)}$$

where R3A4 represents the inhibition ratio of CYP3A4 by ICZ ($CL_{int,3A4}$(+ICZ)/$CL_{int,3A4}$(control)). Assuming that GEM (and its glucuronide) inhibits both OATP1B1 and CYP2C8, the following equations can be derived for the +GEM (co-administration of GEM) condition:

$$AUC_{+GEM} = \frac{Dose_{+GEM}}{R\inf \times fb \cdot PS_{inf} \times \frac{\gamma_{+GEM}}{1+\gamma_{+GEM}}} \quad \text{(Eq. 7)}$$

$$\gamma_{+GEM} = fm_{2C8} \times \gamma \times R2C8 + (1 - fm_{2C8}) \times \gamma \quad \text{(Eq. 8)}$$

where Rinf and R2C8 represents the inhibition ratio of hepatic uptake and CYP2C8, respectively, by GEM (PS_{inf}(+GEM)/PS_{inf}(control) and $CL_{int,2C8}$(+GEM)/$CL_{int,2C8}$(control), respectively). Finally, the AUC and R values can be expressed as follows for the +ICZ+GEM (co-administration of both ICZ and GEM) condition:

$$AUC_{+ICZ+GEM} = \frac{Dose_{+ICZ+GEM}}{R\inf \times fb \cdot PS_{inf} \times \frac{\gamma_{+ICZ+GEM}}{1+\gamma_{+ICZ+GEM}}} \quad \text{(Eq. 9)}$$

$$\gamma_{+ICZ+GEM} = fm_{2C8} \times \gamma \times R2C8 + (1 - fm_{2C8}) \times \gamma \times R3A4 \quad \text{(Eq. 10)}$$

The observed AUC values for the 4 conditions (control, +ICZ, +GEM, and +ICZ+GEM) were analyzed by the above equations using a multipurpose nonlinear

Downloaded from dmd.aspetjournals.org at ASPET Journals on April 19, 2024

DMD Fast Forward. Published on November 8, 2012 as DOI: 10.1124/dmd.112.049460
This article has not been copyedited and formatted. The final version may differ from this version.

least-squares fitting computer program 'Napp' (version 2.26) (Hisaka and Sugiyama, 1998) to obtain the optimized values for Rinf, R2C8, R3A4 and fm_{2C8}, fixing the $f_b \cdot PS_{inf}$ value at 100 L/hr.

3. Fitting analyses of the blood concentration-time profiles of inhibitors (ICZ, GEM and GEM-glu) based on a simple PBPK model

1) ICZ

A simple PBPK model for ICZ disposition, consisting of a blood compartment, a gastrointestinal compartment and a liver compartment, was constructed as shown in Fig. 1A. According to this model, the concentration profile of ICZ can be expressed by the following differential equations:

$$V_{b,icz}\frac{dC_{b,icz}}{dt} = Q_h\frac{R_{b,icz}}{K_{p,icz}}C_{h,icz} - Q_h \cdot C_{b,icz} \quad \text{(Eq. 11)}$$

$$V_h\frac{dC_{h,icz}}{dt} = Q_h \cdot C_{b,icz} - Q_h\frac{R_{b,icz}}{K_{p,icz}}C_{h,icz} - f_{h,icz} \cdot CL_{int,icz} \cdot C_{h,icz} + k_{a,icz} \cdot F_a F_{g,icz} \cdot Dose_{icz} \cdot \exp(-k_{a,icz} \cdot t) \quad \text{(Eq. 12)}$$

where C_b and C_h represent the concentrations in the blood and liver compartments, respectively; V_b represents the distribution volume in the blood compartment; V_h represents the volume of liver; k_a represents the absorption rate constant; R_b represents the blood-to-plasma concentration ratio; K_p represents the liver-to-plasma concentration

Downloaded from dmd.aspetjournals.org at ASPET Journals on April 19, 2024

DMD Fast Forward. Published on November 8, 2012 as DOI: 10.1124/dmd.112.049460
This article has not been copyedited and formatted. The final version may differ from this version.

ratio; and f_h represents the unbound fraction in the liver. The subscript 'icz' after each parameter indicates the parameters for ICZ.

Because the concentration profile of ICZ was not shown in the interaction study with repaglinide (Niemi et al., 2003a), the values of $V_{b,icz}$, $k_{a,icz}$ and $CL_{int,icz}$ were optimized by fitting analyses based on the concentration profile reported in another paper (Jaakkola et al., 2005). The Dose was set at 100,000 μg (Niemi et al., 2003a; Jaakkola et al., 2005), and values of Q_h=86.9 L/hr and V_h=1.22 L were used for physiological parameters (Watanabe et al., 2009). The F_aF_g was estimated by a similar method as that for repaglinide described above using the values of CL_{tot} and bioavailability (Table 1), The f_h value was calculated based on the following equation (Poulin and Theil, 2002):

$$f_p / f_h = 0.5 \times (f_p + 1) \quad \text{(Eq. 13)}$$

where f_p represents the unbound fraction in the plasma. The K_p value was calculated as follows (Poulin and Theil, 2002):

$$K_p = (P \times 0.02289 + 0.72621) / (P \times 0.001719 + 0.960581) \times f_p / f_h \quad \text{(Eq. 14)}$$

$$P = 10^{cLogP} \quad \text{(Eq. 15)}$$

where cLogP represents the logarithm of the computer-calculated partition coefficient between n-octanol and water. The initial ICZ concentration in the blood compartment

Downloaded from dmd.aspetjournals.org at ASPET Journals on April 19, 2024

DMD Fast Forward. Published on November 8, 2012 as DOI: 10.1124/dmd.112.049460
This article has not been copyedited and formatted. The final version may differ from this version.

($C_{b,0}$) after 3 days of repeated oral administration was obtained from the reported concentration profile (Jaakkola et al., 2005). The initial ICZ concentration in the liver compartment ($C_{h,0}$) was assumed to be equal to $C_{b,0} \times K_p / R_b$.

2) GEM and GEM-glu

A simple PBPK model constructed for GEM and GEM-glu disposition, consisting of a blood compartment, a gastrointestinal compartment, a liver extracellular space compartment and a liver compartment for GEM and a blood compartment, a liver extracellular space compartment and a liver compartment for GEM-glu, is shown in Fig. 1B. According to this model, the concentration profiles of GEM and GEM-glu can be expressed by the following differential equations:

$$V_{b,gem}\frac{dC_{b,gem}}{dt} = Q_h \cdot C_{e,gem} - Q_h \cdot C_{b,gem} \quad \text{(Eq. 16)}$$

$$V_e\frac{dC_{e,gem}}{dt} = Q_h \cdot C_{b,gem} - Q_h \cdot C_{e,gem} - f_{b,gem} \cdot PS_{inf,gem} \cdot C_{e,gem} + f_{h,gem} \cdot PS_{eff,gem} \cdot C_{h,gem} + k_{a,gem} \cdot F_a F_{g,gem} \cdot Dose_{gem} \cdot \exp(-k_{a,gem}(t - Lag_{gem})) \quad \text{(Eq. 17)}$$

$$V_h\frac{dC_{h,gem}}{dt} = f_{b,gem} \cdot PS_{inf,gem} \cdot C_{e,gem} - f_{h,gem} \cdot PS_{eff,gem} \cdot C_{h,gem} - (f_{h,gem} \cdot CL_{int1} + f_{h,gem} \cdot CL_{int2})C_{h,gem} \quad \text{(Eq. 18)}$$

$$V_{b,glu}\frac{dC_{b,glu}}{dt} = Q_h \cdot C_{e,glu} - Q_h \cdot C_{b,glu} - CL_{NH,glu} \cdot C_{b,glu} \quad \text{(Eq. 19)}$$

$$V_e\frac{dC_{e,glu}}{dt} = Q_h \cdot C_{b,glu} - Q_h \cdot C_{e,glu} - f_{b,glu} \cdot PS_{inf,glu} \cdot C_{e,glu} + f_{h,glu} \cdot PS_{eff,glu} \cdot C_{h,glu}$$

Downloaded from dmd.aspetjournals.org at ASPET Journals on April 19, 2024

DMD Fast Forward. Published on November 8, 2012 as DOI: 10.1124/dmd.112.049460
This article has not been copyedited and formatted. The final version may differ from this version.

(Eq. 20)

$$V_h \frac{dC_{h,glu}}{dt} = f_{h,gem} \cdot CL_{int1} \cdot C_{h,gem} + f_{b,glu} \cdot PS_{inf,glu} \cdot C_{e,glu} - f_{h,glu} \cdot PS_{eff,glu} \cdot C_{h,glu} - f_{h,glu} \cdot CL_{int,h,glu} \cdot C_{h,glu} \quad \text{(Eq. 21)}$$

where V_e represents the volume of the liver extracellular space (0.469 L) (Watanabe et al., 2009); Lag represents the lag time for absorption of GEM; CL_{int1} and CL_{int2} were defined as the hepatic intrinsic clearances for glucuronidation and other metabolic pathway(s), respectively, for GEM; CL_{NH} represents the non-hapatic clearance for elimination of GEM-glu from the blood compartment; $CL_{int,h}$ represents the hepatic intrinsic clearance for elimination of GEM-glu from the liver compartment. The subscripts 'gem' and 'glu' after each parameter indicate the parameters for GEM and GEM-glu, respectively.

Because the concentration profiles of GEM and GEM-glu were not shown in the interaction study with repaglinide (Niemi et al., 2003a), the values of the PK parameters for GEM and GEM-glu were estimated based on their concentration profiles after repeated oral administration of GEM according to the same dosage schedule, as reported in another paper (Tornio et al., 2008). The Dose was set at 600,000 μg (Niemi et al., 2003a; Tornio et al., 2008), and the F_aF_g for GEM was estimated by a similar method as that for repaglinide described above using the values of CL_{tot} and bioavailability (Table 1). The CL_{int1}/CL_{int2} ratio was fixed at 6.1 (=0.86/0.14) because

Downloaded from dmd.aspetjournals.org at ASPET Journals on April 19, 2024

DMD Fast Forward. Published on November 8, 2012 as DOI: 10.1124/dmd.112.049460
This article has not been copyedited and formatted. The final version may differ from this version.

the fraction of GEM metabolized by the UDP-glucuronosyltransferase is reported to be 0.86 (Kilford et al., 2009). The $PS_{inf,gem}$ was assumed to be equal to 10-fold the value of $CL_{int,all}$ for GEM that was calculated by Eq. 1 using the reported AUC value (Tornio et al., 2008); the $PS_{inf,glu}$ was calculated based on an assumption that $fb \cdot PS_{inf,glu}$ was equal to $fb \cdot PS_{inf,gem}$; the $CL_{NH,glu}$ was assumed to be equal to the value of the glomerular filtration rate (Davies and Morris, 1993) multiplied by $f_{b,glu}$. Initially, the GEM blood concentration profile was fitted to Eq. 16 based on the simultaneous analysis of Eqs. 16-18 to obtain the optimized values of $k_{a,gem}$, $V_{b,gem}$, $PS_{eff,gem}$ and CL_{int1}. Then, fixing the above parameters for GEM at the optimized values, the GEM-glu blood concentration profile was fitted to Eq. 19 based on the simultaneous analysis of Eqs. 19-21 to obtain the optimized values of $PS_{eff,glu}$ and $CL_{int,h,glu}$.

4. Fitting analyses of repaglinide concentration profiles based on a simple PBPK model

A simple PBPK model constructed for repaglinide disposition, consisting of a blood compartment, a gastrointestinal compartment, a peripheral compartment, a liver extracellular space compartment and a liver compartment, is shown in Fig. 1C. According to this model, the concentration profile of repaglinide can be expressed by the following differential equations considering the inhibition of hepatic uptake by

Downloaded from dmd.aspetjournals.org at ASPET Journals on April 19, 2024

DMD Fast Forward. Published on November 8, 2012 as DOI: 10.1124/dmd.112.049460
This article has not been copyedited and formatted. The final version may differ from this version.

GEM and GEM-glu, a mechanism-based inhibition of CYP2C8 by GEM-glu and a competitive inhibition of CYP3A4 by ICZ:

$$V_{b,s}\frac{dC_{b,s}}{dt} = Q_h \cdot C_{e,s} - Q_h \cdot C_{b,s} - k_{12,s} \cdot V_{b,s} \cdot C_{b.s} + k_{21,s} \cdot X_{sub} \quad \text{(Eq. 22)}$$

$$V_e\frac{dC_{e,s}}{dt} = Q_h \cdot C_{b,s} - Q_h \cdot C_{e,s} - \frac{f_{b,s} \cdot PS_{inf,s}}{1 + \frac{f_{b,gem} \cdot C_{e,gem}}{K_{i,1B1,gem}} + \frac{f_{b,glu} \cdot C_{e,glu}}{K_{i,1B1,glu}}} C_{e,s} + f_{h,s} \cdot PS_{eff,s} \cdot C_{h,s} + k_{a,s} \cdot F_a F_{g,s} \cdot Dose_s \cdot \exp(-k_{a,s}(t - Lag_s)) \quad \text{(Eq. 23)}$$

$$V_h\frac{dC_{h,s}}{dt} = \frac{f_{b,s} \cdot PS_{inf,s}}{1 + \frac{f_{b,gem} \cdot C_{e,gem}}{K_{i,1B1,gem}} + \frac{f_{b,glu} \cdot C_{e,glu}}{K_{i,1B1,glu}}} C_{e,s} - f_{h,s} \cdot PS_{eff,s} \cdot C_{h,s} - f_{h,s} \cdot CL_{int,s}\left\{ fm_{2C8} \cdot RE_{act,2C8} + \frac{1 - fm_{2C8}}{1 + \frac{f_{h,icz} \cdot C_{h,icz}}{K_{i,3A4,icz}}} \right\} C_{h,s} \quad \text{(Eq. 24)}$$

$$\frac{dX_{sub}}{dt} = k_{12,s} \cdot V_{b,s} \cdot C_{b,s} - k_{21,s} \cdot X_{sub} \quad \text{(Eq. 25)}$$

where the subscript 's' after each parameter indicates the parameters for repaglinide; X_{sub} represents the amount of repaglinide in the peripheral compartment; k_{12} and k_{21} represent the transfer rate constant from the blood compartment to the peripheral compartment and that from the peripheral compartment to the blood compartment, respectively; $K_{i,1B1}$ and $K_{i,3A4}$ represent the inhibition constant for hepatic uptake and that for CYP3A4-mediated hepatic metabolism, respectively. It was assumed that the inhibition of hepatic uptake and metabolism depends on the inhibitor concentration in the liver extracellular space compartment (C_e) and that in the liver compartment (C_h),

Downloaded from dmd.aspetjournals.org at ASPET Journals on April 19, 2024

DMD Fast Forward. Published on November 8, 2012 as DOI: 10.1124/dmd.112.049460
This article has not been copyedited and formatted. The final version may differ from this version.

respectively. Lag for repaglinide was assumed in the present analysis to include the 1 hr lag time between the doses of ICZ/GEM and repaglinide (Niemi et al., 2003a).

The differential equation for $REact_{2C8}$, the fraction of active CYP2C8, can be expressed as follows considering the mechanism-based inhibition by GEM-glu:

$$\frac{dRE_{act,2C8}}{dt} = -\frac{k_{inact.2C8} \cdot RE_{act,2C8} \cdot f_{h,glu} \cdot C_{h,glu}}{K_{i,app,2C8} + f_{h,glu} \cdot C_{h,glu}} + k_{deg,2C8}(1 - RE_{act,2C8}) \quad \text{(Eq. 26)}$$

where $k_{inact,2C8}$ and $K_{i,app,2C8}$ represent the maximum inactivation rate constant and the apparent inhibition constant, respectively, and $k_{deg,2C8}$ represents the first-order rate constant for degradation of CYP2C8.

The repaglinide blood concentration profiles for the 4 conditions (control, +ICZ, +GEM, and +ICZ+GEM) were fitted to Eq. 22 based on the simultaneous analysis of Eqs. 11, 12 and Eqs. 16-26 to obtain the optimized values of $k_{a,s}$, Lag_s, $V_{b,s}$, $f_{b,s} \cdot PS_{inf,s}$, $f_{h,s} \cdot CL_{int,s}$, $k_{12,s}$, $k_{21,s}$, $K_{i,3A4,icz}$ and $K_{i,1B1,gem}$. The Dose of repaglinide was set at 250 μg, which is the oral dose used in the reported interaction study (Niemi et al., 2003a); the values of $K_{i,app,2C8}$, $k_{inact,2C8}$ and $k_{deg,2C8}$ were fixed at the reported values (20 μM, 12.6 hr^{-1} and 0.030 hr^{-1}, respectively) (Ogilvie et al., 2006; Yang et al., 2008); the ratio of $K_{i,1B1,glu}/K_{i,1B1,gem}$ was fixed at the mean of the reported values obtained in in vitro uptake studies using human hepatocytes and OATP1B1-expressing cells (0.385) (Shitara et al., 2004; Nakagomi-Hagihara et al., 2007); the values of $PS_{eff,s}$ was

Downloaded from dmd.aspetjournals.org at ASPET Journals on April 19, 2024

DMD Fast Forward. Published on November 8, 2012 as DOI: 10.1124/dmd.112.049460
This article has not been copyedited and formatted. The final version may differ from this version.

calculated as the geometric mean of the reported intrinsic clearances for passive diffusion of repaglinide into human and rat hepatocytes (Yabe et al., 2011; Ménochet et al., 2012; Jones et al., 2012) (Table 2). The PK parameters for ICZ, GEM and GEM-glu were fixed at the values obtained by the above-mentioned analyses of respective concentration profiles (Table 1).

5. Simulation of the repaglinide concentration profiles in other interaction studies with GEM

Simulation studies were performed to investigate whether the repaglinide concentration increase produced by concomitant GEM administration at various timing/doses, reported in other papers, can be reproduced using the same PBPK model (Figs. 1B and 1C, Eqs. 16-26) together with the parameters estimated in the present study (Table 2). The following 3 studies were investigated:

Report 1: Repaglinide was taken 1, 24, 48, or 96 hr after the last administration of gemfibrozil (600 mg, p.o., b.i.d., for 3 days) (Backman et al., 2009).

Report 2: Repaglinide was taken 0, 1, 3, or 6 hr after a single administration of gemfibrozil (600 mg, p.o.) (Honkalammi et al., 2011).

Report 3: Repaglinide was taken 1 hr after the last administration of gemfibrozil (30,

Downloaded from dmd.aspetjournals.org at ASPET Journals on April 19, 2024

DMD Fast Forward. Published on November 8, 2012 as DOI: 10.1124/dmd.112.049460
This article has not been copyedited and formatted. The final version may differ from this version.

100, or 600 mg, p.o., b.i.d., for 3 days) (Honkalammi et al., 2012).

6. Analysis

A multipurpose nonlinear least-squares fitting computer program 'Napp' (version 2.26) (Hisaka and Sugiyama, 1998) was used for all the fitting and simulation analyses. The differential equations were numerically solved by using the Runge-Kutta-Fehlberg method. The fitting analysis was carried out based on a nonlinear least-squares procedure with a weight value fixed at 1.

Downloaded from dmd.aspetjournals.org at ASPET Journals on April 19, 2024

DMD Fast Forward. Published on November 8, 2012 as DOI: 10.1124/dmd.112.049460
This article has not been copyedited and formatted. The final version may differ from this version.

Results

Analysis of the increased repaglinide AUC produced by ICZ and GEM

The inhibition ratios of repaglinide intrinsic clearances as well as the fm_{2C8} were estimated by regression analysis of the AUC increase by ICZ and GEM using Eqs. 4-10. The R3A4, R2C8, Rinf and fm_{2C8} were optimized at 0.22, 0.045, 0.50 and 0.85, respectively, showing that the reported AUC increase for each condition (control, +ICZ, +GEM, and +ICZ+GEM) can be explained by the CYP3A4, CYP2C8 and OATP1B1 all being inhibited by co-administration of ICZ and GEM. The estimated fm_{2C8} value was used as its initial value in the final fitting analysis of the repaglinide concentration profiles.

Analysis of the ICZ concentration profile

The blood concentration profile of ICZ was fitted to Eq. 11 based on the simple PBPK model (Fig. 1A) and the values of $k_{a,icz}$, $V_{b,icz}$ and $CL_{int,icz}$ were optimized to best fit the observed concentration profile. All the parameters for ICZ used in the analyses are summarized in Table 1 together with the estimated values. As shown in Fig. 2A, the obtained concentration profile of ICZ after 3 days of repeated administration was close to the observed values (Jaakkola et al., 2005).

Downloaded from dmd.aspetjournals.org at ASPET Journals on April 19, 2024

DMD Fast Forward. Published on November 8, 2012 as DOI: 10.1124/dmd.112.049460
This article has not been copyedited and formatted. The final version may differ from this version.

Analysis of the GEM and GEM-glu concentration profiles

The blood concentration profiles of GEM and GEM-glu were fitted to Eq. 16 and Eq. 19, respectively, based on the simple PBPK model (Fig. 1B) and the values of $k_{a,gem}$, $V_{b,gem}$, $PS_{eff,gem}$, $PS_{eff,glu}$, CL_{int1} and $CL_{int,h,glu}$ were optimized to best fit the observed concentration profiles. All parameters used in the analysis are summarized in Table 1 together with the estimated values. As shown in Fig. 2B, the obtained concentration profiles of GEM and GEM-glu after 3 days of repeated administration of GEM were close to the observed values (Tornio et al., 2008).

Analysis of the repaglinide concentration profiles considering the interaction with ICZ/GEM

The blood concentration profiles of repaglinide for the 4 conditions (control, +ICZ, +GEM, and +ICZ+GEM) were analyzed based on the simple PBPK model (Fig. 1C) and differential equations (Eqs. 22-26) together with the concentration profiles of ICZ, GEM and GEM-glu (Eqs. 11, 12, 16-21). The values of $k_{a,s}$, $V_{b,s}$, $k_{12,s}$, $k_{21,s}$, Lag_s, fm_{2C8}, $K_{i,3A4,icz}$ and $K_{i,1B1,gem}$ were optimized by simultaneous fitting analysis fixing all the parameters for the inhibitors (ICZ, GEM and GEM-glu) at values shown in Table 1. All

Downloaded from dmd.aspetjournals.org at ASPET Journals on April 19, 2024

DMD Fast Forward. Published on November 8, 2012 as DOI: 10.1124/dmd.112.049460
This article has not been copyedited and formatted. The final version may differ from this version.

the parameters for repaglinide used in the analyses are summarized in Table 2 together with the estimated values. The obtained concentration profiles of repaglinide were close to the observed values for each of the 4 conditions as shown in Fig. 2C. The repaglinide AUC ratios for +ICZ, +GEM and +ICZ＋GEM conditions were calculated to be 1.2-, 6.5-, 24.3-fold, respectively.

Simulation of the repaglinide concentration profiles in other interaction studies with GEM

The repaglinide concentration increase produced by GEM reported in other interaction studies (Backman et al., 2009; Honkalammi et al., 2011; Honkalammi et al., 2012) were simulated based on the same PBPK model (Figs. 1B and 1C; Eqs. 16-26) together with the parameters estimated in the present study (Table 2). Fig. 3 shows the observed (Backman et al., 2009) and simulated concentration profiles of repaglinide administered at various intervals after repeated GEM dosing. The persistent interaction, which recovers after 96 hr, was well reproduced in our simulation analysis. Furthermore, the estimated AUC increase agreed well with the observed values for all the conditions investigated (Table 3).

Downloaded from dmd.aspetjournals.org at ASPET Journals on April 19, 2024

DMD Fast Forward. Published on November 8, 2012 as DOI: 10.1124/dmd.112.049460
This article has not been copyedited and formatted. The final version may differ from this version.

Discussion

The AUC of repaglinide has been reported to be increased 1.4-, 8.1- or 19.4-fold when healthy volunteers received repaglinide after 3 days of treatment with ICZ, GEM, or both GEM and ICZ, respectively (Niemi et al., 2003a). The present study investigated whether these interactions can be quantitatively explained by the inhibition of the transporter and enzymes involved in repaglinide disposition, based on the clearance concept and simple PBPK modeling.

The major route of repaglinide elimination from the body is hepatic metabolism, with a negligible contribution from renal clearance (f_e = 0.001) (van Heiningen et al., 1999), and the plasma concentration profile of repaglinide has been shown to be affected by the genetic polymorphism of OATP1B1 (Niemi et al., 2005; Kalliokoski et al., 2008) or CYP2C8 (Niemi et al., 2003b; Niemi et al., 2005). In the present analysis, therefore, it was assumed that repaglinide is eliminated only from the liver and that both hepatic uptake and metabolism contribute to its hepatic elimination. As a result, the β value in Eq. 2 was calculated to be 0.27 using the optimized values of PS_{eff} and CL_{int} (Table 2), which indicates that its hepatic elimination is not completely limited by the hepatic uptake.

It has been reported that about 66% of orally administered [^{14}C]-repaglinide is

Downloaded from dmd.aspetjournals.org at ASPET Journals on April 19, 2024

DMD Fast Forward. Published on November 8, 2012 as DOI: 10.1124/dmd.112.049460
This article has not been copyedited and formatted. The final version may differ from this version.

excreted as a metabolite M2 in the feces and urine in healthy volunteers (van Heiningen et al., 1999). In *in vitro* studies, M0-OH, M1, M2, M4 and M5 have been reported as metabolites of repaglinide (Bidstrup et al., 2003). At a relatively high concentration of repaglinide (22 μM), formation of M1 by CYP3A4 and M4 by CYP2C8 were the major metabolic pathways in human liver microsomes (Bidstrup et al., 2003). Kajosaari et al. investigated the contributions of CYP3A4 and CYP2C8 to the metabolism of repaglinide at a therapeutic repaglinide concentration (<0.4 μM) using recombinant enzymes but the results were highly dependent on the scaling factor used (Kajosaari et al., 2005a). It has also been reported recently that the fm_{2C8} value was estimated to be 0.49, 0.41 and 0.63 in an in vitro study using human hepatocytes, S9 fractions and liver microsomes, respectively (Säll et al., 2012). In the present study, the estimated fm_{2C8} value of 0.801 (Table 2) indicates a larger contribution of CYP2C8 than CYP3A4, which is consistent with the previous findings that the AUC of repaglinide was affected by the genetic polymorphism of CYP2C8 (Niemi et al., 2003b; Niemi et al., 2005) but not CYP3A4 (Ruzilawati and Gan, 2010).

In vitro studies have demonstrated that both GEM and GEM-glu inhibit OATP1B1 (Shitara et al., 2004; Nakagomi-Hagihara et al., 2007; Hinton et al., 2008). The K_i or IC_{50} values for GEM and of GEM-glu were reported to be 72.4 μM and 24.3 μM,

Downloaded from dmd.aspetjournals.org at ASPET Journals on April 19, 2024

DMD Fast Forward. Published on November 8, 2012 as DOI: 10.1124/dmd.112.049460
This article has not been copyedited and formatted. The final version may differ from this version.

respectively, in OATP1B1-expressing MDCK cells (Shitara et al., 2004); 35.8 μM and 9.3 μM, respectively, in human hepatocytes (Nakagomi-Hagihara et al., 2007); and 15.5 μM and 7.9 μM, respectively, in OATP1B1-expressing Xenopus oocytes (Nakagomi-Hagihara et al., 2007). In the present fitting analysis, the ratio of $K_{i,1B1glu}$ to $K_{i,1B1gem}$ was fixed at 0.385, the mean ratio calculated from these reported values (0.26 - 0.51), to reduce the number of unknown parameters. As a result, the estimated K_i values ($K_{i,1B1gem}$ = 14.2±10.1 μM, $K_{i,1B1glu}$ = 5.48 μM) (Table 2) were close to the reported values described above.

Although both GEM and GEM-glu have been also reported to inhibit CYP2C8, the IC_{50} value for GEM was 7-fold higher than that for GEM-glu (Shitara et al., 2004) which was shown to be a mechanism-based inhibitor of CYP2C8 (Ogilvie et al., 2006). In the present study, therefore, only the mechanism-based inhibition of CYP2C8 by GEM-glu was incorporated in the model fixing the $k_{inact,2C8}$ and $K_{i,app,2C8}$ at the reported values (12.6 hr^{-1} and 52 μM, respectively) (Ogilvie et al., 2006).

Based on a PBPK analysis of reported in vivo interactions between ICZ and CYP3A4 substrates, Kato et al. have reported an in vivo K_i value of 0.282 μg/L (0.4 nM) for ICZ against CYP3A4, which is nearly 500-fold lower than the average K_i value obtained in in vitro studies using human liver microsomes (Kato et al., 2008). The

Downloaded from dmd.aspetjournals.org at ASPET Journals on April 19, 2024

DMD Fast Forward. Published on November 8, 2012 as DOI: 10.1124/dmd.112.049460
This article has not been copyedited and formatted. The final version may differ from this version.

$K_{i,3A4,icz}$ value of 0.0477±0.0365 μg/L (0.0676±0.0518 nM) estimated by the present fitting analysis (Table 2) was even smaller than the reported in vivo K_i value, although the contribution of CYP3A4 inhibition to the overall change in repaglinide pharmacokinetics should not be large in the present analysis based on the fm_{2C8} value of 0.801 and the hepatic disposition limited in part by the uptake ($\beta = 0.27$).

In order to confirm the validity of the parameter values obtained in the present study, sensitivity analyses were carried out for fm_{2C8}, $K_{i,1B1,gem}$ and $K_{i,3A4,icz}$. As shown in Fig. 4, the simulated concentration profiles of repaglinide deviated greatly from the observed concentrations when altered values of fm_{2C8} and K_i were used, suggesting the reliability of these parameters estimated in the present analysis. Furthermore, the repaglinide concentration increase by concomitant GEM administration at various timings/doses, reported in other papers, were well reproduced using the same PBPK model together with the parameters estimated in the present study (Fig. 3 and Table 3). These results indicate the validity of the PBPK model used in the present analyses as well as the estimated parameters.

In conclusion, the plasma concentration profiles of repaglinide in the interaction study were reproduced by the PBPK model, suggesting that the reported concentration increase by ICZ and GEM results from the inhibition of OATP1B1-mediated hepatic

Downloaded from dmd.aspetjournals.org at ASPET Journals on April 19, 2024

DMD Fast Forward. Published on November 8, 2012 as DOI: 10.1124/dmd.112.049460
This article has not been copyedited and formatted. The final version may differ from this version.

uptake by GEM and GEM-glu and that of CYP2C8- and CYP3A4-mediated metabolism by GEM-glu and ICZ, respectively. The present PBPK model is expected to be applicable to the analyses of other interactions involving both hepatic uptake transporters and metabolic enzymes.

Downloaded from dmd.aspetjournals.org at ASPET Journals on April 19, 2024

DMD Fast Forward. Published on November 8, 2012 as DOI: 10.1124/dmd.112.049460
This article has not been copyedited and formatted. The final version may differ from this version.

Authorship Contribution

Participated in research design: Kudo, Sugiyama, Ito

Conducted experiments: Kudo, Ito

Contributed new reagents or analytic tools: Hisaka

Performed data analysis: Kudo, Hisaka, Sugiyama, Ito

Wrote or contributed to the writing of the manuscript: Kudo, Hisaka, Sugiyama, Ito

Downloaded from dmd.aspetjournals.org at ASPET Journals on April 19, 2024

DMD Fast Forward. Published on November 8, 2012 as DOI: 10.1124/dmd.112.049460
This article has not been copyedited and formatted. The final version may differ from this version.

References

Backman JT, Kivistö KT, Olkkola KT, and Neuvonen PJ (1998) The area under the plasma concentration-time curve for oral midazolam is 400-fold larger during treatment with itraconazole than with rifampicin. *Eur J Clin Pharmacol* **54:** 53-58.

Backman JT, Kyrklund C, Neuvonen M, and Neuvonen PJ (2002) Gemfibrozil greatly increases plasma concentrations of cerivastatin. *Clin Pharmacol Ther* **72:** 685-691.

Backman JT, Honkalammi J, Neuvonen M, Kurkinen KJ, Tornio A, Niemi M, and Neuvonen PJ (2009) CYP2C8 activity recovers within 96 hours after gemfibrozil dosing: estimation of CYP2C8 half-life using repaglinide as an in vivo probe. *Drug Metab Dispos* **37:** 2359-2366.

Bidstrup TB, Bjørnsdottir I, Sidelmann UG, Thomsen MS, and Hansen KT (2003) CYP2C8 and CYP3A4 are the principal enzymes involved in the human in vitro biotransformation of the insulin secretagogue repaglinide. *Br J Clin Pharmacol* **56:** 305-314.

Bidstrup TB, Stilling N, Damkier P, Scharling B, Thomsen MS, and Brøsen K (2004) Rifampicin seems to act as both an inducer and an inhibitor of the metabolism of repaglinide. *Eur J Clin Pharmacol* **60:** 109-114.

Davies B and Morris T (1993) Physiological parameters in laboratory animals and

Downloaded from dmd.aspetjournals.org at ASPET Journals on April 19, 2024

DMD Fast Forward. Published on November 8, 2012 as DOI: 10.1124/dmd.112.049460
This article has not been copyedited and formatted. The final version may differ from this version.

humans. *Pharm Res* **10:** 1093-1095.

Fuhlendorff J, Rorsman P, Kofod H, Brand CL, Rolin B, MacKay P, Shymko R, and Carr RD (1998) Stimulation of insulin release by repaglinide and glibenclamide involves both common and distinct processes. *Diabetes* **47:** 345-351.

Galetin A, Ito K, Hallifax D, and Houston JB (2005) CYP3A4 substrate selection and substitution in the prediction of potential drug-drug interactions. *J Pharmacol Exp Ther* **314:** 180-190.

Hatorp V (2002) Clinical pharmacokinetics and pharmacodynamics of repaglinide. *Clin Pharmacokinet* **41:** 471-483.

Hinton LK, Galetin A, and Houston JB (2008) Multiple inhibition mechanisms and prediction of drug-drug interactions: status of metabolism and transporter models as exemplified by gemfibrozil-drug interactions. *Pharm Res* **25:** 1063-1074.

Hisaka A and Sugiyama Y (1998) Analysis of nonlinear and nonsteady state hepatic extraction with the dispersion model using the finite difference method. *J Pharmacokinet Biopharm* **26:** 495-519.

Honkalammi J, Niemi M, Neuvonen PJ, and Backman JT (2011) Mechanism-based inactivation of CYP2C8 by gemfibrozil occurs rapidly in humans. *Clin Pharmacol Ther* **89:** 579-586.

Downloaded from dmd.aspetjournals.org at ASPET Journals on April 19, 2024

DMD Fast Forward. Published on November 8, 2012 as DOI: 10.1124/dmd.112.049460
This article has not been copyedited and formatted. The final version may differ from this version.

Honkalammi J, Niemi M, Neuvonen PJ, and Backman JT (2012) Gemfibrozil is a strong inactivator of CYP2C8 in very small multiple doses. *Clin Pharmacol Ther* **91:** 846-855.

Ito K, Ogihara K, Kanamitsu S, and Itoh T (2003) Prediction of the in vivo interaction between midazolam and macrolides based on in vitro studies using human liver microsomes. *Drug Metab Dispos* **31:** 945-954.

Jaakkola T, Backman JT, Neuvonen M, and Neuvonen PJ (2005) Effects of gemfibrozil, itraconazole, and their combination on the pharmacokinetics of pioglitazone. *Clin Pharmacol Ther* **77:** 404-414.

Jones HM, Barton HA, Lai Y, Bi YA, Kimoto E, Kempshall S, Tate SC, El-Kattan A, Houston JB, Galetin A, and Fenner KS (2012) Mechanistic pharmacokinetic modeling for the prediction of transporter-mediated disposition in humans from sandwich culture human hepatocyte data. *Drug Metab Dispos* **40:** 1007-1017.

Kajosaari LI, Laitila J, Neuvonen PJ, and Backman JT (2005a) Metabolism of repaglinide by CYP2C8 and CYP3A4 in vitro: effect of fibrates and rifampicin. *Basic Clin Pharmacol Toxicol* **97:** 249-256.

Kajosaari LI, Niemi M, Neuvonen M, Laitila J, Neuvonen PJ, and Backman JT (2005b) Cyclosporine markedly raises the plasma concentrations of repaglinide. *Clin*

Downloaded from dmd.aspetjournals.org at ASPET Journals on April 19, 2024

DMD Fast Forward. Published on November 8, 2012 as DOI: 10.1124/dmd.112.049460
This article has not been copyedited and formatted. The final version may differ from this version.

Pharmacol Ther **78:** 388-399.

Kajosaari LI, Niemi M, Backman JT, and Neuvonen PJ (2006) Telithromycin, but not montelukast, increases the plasma concentrations and effects of the cytochrome P450 3A4 and 2C8 substrate repaglinide. *Clin Pharmacol Ther* **79:** 231-242.

Kalliokoski A, Backman JT, Kurkinen KJ, Neuvonen PJ, and Niemi M (2008) Effects of gemfibrozil and atorvastatin on the pharmacokinetics of repaglinide in relation to SLCO1B1 polymorphism. *Clin Pharmacol Ther* **84:** 488-496.

Kanamitsu S, Ito K, and Sugiyama Y (2000) Quantitative prediction of in vivo drug-drug interactions from in vitro data based on physiological pharmacokinetics: use of maximum unbound concentration of inhibitor at the inlet to the liver. *Pharm Res* **17:** 336-343.

Kato M, Shitara Y, Sato H, Yoshisue K, Hirano M, Ikeda T, and Sugiyama Y (2008) The quantitative prediction of CYP-mediated drug interaction by physiologically based pharmacokinetic modeling. *Pharm Res* **25:** 1891-1901.

Kilford PJ, Stringer R, Sohal B, Houston JB, and Galetin A (2009) Prediction of drug clearance by glucuronidation from in vitro data: use of combined cytochrome P450 and UDP-glucuronosyltransferase cofactors in alamethicin-activated human liver microsomes. *Drug Metab Dispos* **37:** 82-89.

Downloaded from dmd.aspetjournals.org at ASPET Journals on April 19, 2024

DMD Fast Forward. Published on November 8, 2012 as DOI: 10.1124/dmd.112.049460
This article has not been copyedited and formatted. The final version may differ from this version.

Kyrklund C, Backman JT, Neuvonen M, and Neuvonen PJ (2003) Gemfibrozil increases plasma pravastatin concentrations and reduces pravastatin renal clearance. *Clin Pharmacol Ther* **73:** 538-544.

Ménochet K, Kenworthy KE, Houston JB, and Galetin A (2012) Use of mechanistic modeling to assess interindividual variability and interspecies differences in active uptake in human and rat hepatocytes. *Drug Metab Dispos* **40:** 1744-1756.

Nakagomi-Hagihara R, Nakai D, Tokui T, Abe T, and Ikeda T (2007) Gemfibrozil and its glucuronide inhibit the hepatic uptake of pravastatin mediated by OATP1B1. *Xenobiotica* **37:** 474-486.

Niemi M, Backman JT, Neuvonen M, Neuvonen PJ, and Kivistö KT (2000) Rifampin decreases the plasma concentrations and effects of repaglinide. *Clin Pharmacol Ther* **68:** 495-500.

Niemi M, Neuvonen PJ, and Kivistö KT (2001) The cytochrome P4503A4 inhibitor clarithromycin increases the plasma concentrations and effects of repaglinide. *Clin Pharmacol Ther* **70:** 58-65.

Niemi M, Backman JT, Neuvonen M, and Neuvonen PJ (2003a) Effects of gemfibrozil, itraconazole, and their combination on the pharmacokinetics and pharmacodynamics of repaglinide: potentially hazardous interaction between gemfibrozil and

Downloaded from dmd.aspetjournals.org at ASPET Journals on April 19, 2024

DMD Fast Forward. Published on November 8, 2012 as DOI: 10.1124/dmd.112.049460
This article has not been copyedited and formatted. The final version may differ from this version.

repaglinide. *Diabetologia* **46:** 347-351.

Niemi M, Leathart JB, Neuvonen M, Backman JT, Daly AK, and Neuvonen PJ (2003b) Polymorphism in CYP2C8 is associated with reduced plasma concentrations of repaglinide. *Clin Pharmacol Ther* **74:** 380-387.

Niemi M, Kajosaari LI, Neuvonen M, Backman JT, and Neuvonen PJ (2004) The CYP2C8 inhibitor trimethoprim increases the plasma concentrations of repaglinide in healthy subjects. *Br J Clin Pharmacol* **57:** 441-447.

Niemi M, Backman JT, Kajosaari LI, Leathart JB, Neuvonen M, Daly AK, Eichelbaum M, Kivistö KT, and Neuvonen PJ (2005) Polymorphic organic anion transporting polypeptide 1B1 is a major determinant of repaglinide pharmacokinetics. *Clin Pharmacol Ther* **77:** 468-478.

Ogilvie BW, Zhang D, Li W, Rodrigues AD, Gipson AE, Holsapple J, Toren P, and Parkinson A (2006) Glucuronidation converts gemfibrozil to a potent, metabolism-dependent inhibitor of CYP2C8: implications for drug-drug interactions. *Drug Metab Dispos* **34:** 191-197.

Poulin P and Theil FP (2002) Prediction of pharmacokinetics prior to in vivo studies. II. Generic physiologically based pharmacokinetic models of drug disposition. *J Pharm Sci* **91:** 1358-1370.

Downloaded from dmd.aspetjournals.org at ASPET Journals on April 19, 2024

DMD Fast Forward. Published on November 8, 2012 as DOI: 10.1124/dmd.112.049460
This article has not been copyedited and formatted. The final version may differ from this version.

Rowland-Yeo K, Jamei M, Yang J, Tucker GT, and Rostami-Hodjegan A (2010) Physiologically based mechanistic modelling to predict complex drug-drug interactions involving simultaneous competitive and time-dependent enzyme inhibition by parent compound and its metabolite in both liver and gut - the effect of diltiazem on the time-course of exposure to triazolam. *Eur J Pharm Sci* **39:** 298-309.

Ruzilawati AB and Gan SH (2010) CYP3A4 genetic polymorphism influences repaglinide's pharmacokinetics. *Pharmacology* **85:** 357-364.

Säll C, Houston JB, and Galetin A (2012) A comprehensive assessment of repaglinide metabolic pathways: impact of choice of in vitro system and relative enzyme contribution to in vitro clearance. *Drug Metab Dispos* **40:** 1279-1289.

Schneck DW, Birmingham BK, Zalikowski JA, Mitchell PD, Wang Y, Martin PD, Lasseter KC, Brown CD, Windass AS, and Raza A (2004) The effect of gemfibrozil on the pharmacokinetics of rosuvastatin. *Clin Pharmacol Ther* **75:** 455-463.

Shitara Y, Hirano M, Sato H, and Sugiyama Y (2004) Gemfibrozil and its glucuronide inhibit the organic anion transporting polypeptide 2 (OATP2/OATP1B1:SLC21A6)-mediated hepatic uptake and CYP2C8-mediated metabolism of cerivastatin: analysis of the mechanism of the clinically relevant

Downloaded from dmd.aspetjournals.org at ASPET Journals on April 19, 2024

DMD Fast Forward. Published on November 8, 2012 as DOI: 10.1124/dmd.112.049460
This article has not been copyedited and formatted. The final version may differ from this version.

drug-drug interaction between cerivastatin and gemfibrozil. *J Pharmacol Exp Ther* **311:** 228-236.

Shitara Y, Horie T, and Sugiyama Y (2006) Transporters as a determinant of drug clearance and tissue distribution. *Eur J Pharm Sci* **27:** 425-446.

Thummel KE, Shen DD, and Isoherranen N (2011) Appendix II. Design and Optimization of Dosage Regimens: Pharmacokinetic Data. *Goodman & Gilman's The Pharmacological Basis of Therapeutics*, 12th ed. (Brunton LL, Chabner BA, and Knollmann BC eds), McGraw-Hill, New York.

Tornio A, Niemi M, Neuvonen M, Laitila J, Kalliokoski A, Neuvonen PJ, and Backman JT (2008) The effect of gemfibrozil on repaglinide pharmacokinetics persists for at least 12 h after the dose: evidence for mechanism-based inhibition of CYP2C8 in vivo. *Clin Pharmacol Ther* **84:** 403-411.

van Heiningen PN, Hatorp V, Kramer Nielsen K, Hansen KT, van Lier JJ, De Merbel NC, Oosterhuis B, and Jonkman JH (1998) Absorption, metabolism and excretion of a single oral dose of (14)C-repaglinide during repaglinide multiple dosing. *Eur J Clin Pharmacol* **55:** 521-525.

Varhe A, Olkkola KT and Neuvonen PJ (1994) Oral triazolam is potentially hazardous to patients receiving systemic antimycotics ketoconazole or itraconazole. *Clin*

Downloaded from dmd.aspetjournals.org at ASPET Journals on April 19, 2024

DMD Fast Forward. Published on November 8, 2012 as DOI: 10.1124/dmd.112.049460
This article has not been copyedited and formatted. The final version may differ from this version.

Pharmacol Ther **56:** 601-607.

von Moltke LL, Greenblatt DJ, Schmider J, Duan SX, Wright CE, Harmatz JS, and Shader RI (1996) Midazolam hydroxylation by human liver microsomes in vitro: inhibition by fluoxetine, norfluoxetine, and by azole antifungal agents. *J Clin Pharmacol* **36:** 783-91.

Wang JS, Neuvonen M, Wen X, Backman JT, and Neuvonen PJ (2002) Gemfibrozil inhibits CYP2C8-mediated cerivastatin metabolism in human liver microsomes. *Drug Metab Dispos* **30:** 1352-1356.

Watanabe T, Kusuhara H, Maeda K, Shitara Y, and Sugiyama Y (2009) Physiologically based pharmacokinetic modeling to predict transporter-mediated clearance and distribution of pravastatin in humans. *J Pharmacol Exp Ther* **328:** 652-662.

Yabe Y, Galetin A, and Houston JB (2011) Kinetic characterization of rat hepatic uptake of 16 actively transported drugs. *Drug Metab Dispos* **39:** 1808-1814.

Yang J, Liao M, Shou M, Jamei M, Yeo KR, Tucker GT, and Rostami-Hodjegan A (2008) Cytochrome p450 turnover: regulation of synthesis and degradation, methods for determining rates, and implications for the prediction of drug interactions. *Curr Drug Metab* **9:** 384-394.

Yoshida K, Maeda K, and Sugiyama Y (2012) Transporter-Mediated Drug-Drug

Downloaded from dmd.aspetjournals.org at ASPET Journals on April 19, 2024

DMD Fast Forward. Published on November 8, 2012 as DOI: 10.1124/dmd.112.049460
This article has not been copyedited and formatted. The final version may differ from this version.

Interactions Involving OATP Substrates: Predictions Based on In Vitro Inhibition Studies. *Clin Pharmacol Ther* **91:** 1053-1064.

Zhang X, Quinney SK, Gorski JC, Jones DR, and Hall SD (2009) Semiphysiologically based pharmacokinetic models for the inhibition of midazolam clearance by diltiazem and its major metabolite. *Drug Metab Dispos* **37:** 1587-1597.

Zhao P, Vieira Mde L, Grillo JA, Song P, Wu TC, Zheng JH, Arya V, Berglund EG, Atkinson AJ Jr, Sugiyama Y, Pang KS, Reynolds KS, Abernethy DR, Zhang L, Lesko LJ, and Huang SM (2012) Evaluation of exposure change of nonrenally eliminated drugs in patients with chronic kidney disease using physiologically based pharmacokinetic modeling and simulation. *J Clin Pharmacol* **52:** 91S-108S.

Downloaded from dmd.aspetjournals.org at ASPET Journals on April 19, 2024

DMD Fast Forward. Published on November 8, 2012 as DOI: 10.1124/dmd.112.049460
This article has not been copyedited and formatted. The final version may differ from this version.

Footnotes

This work was supported by JSPS KAKENHI Grant Number [23590204].

Downloaded from dmd.aspetjournals.org at ASPET Journals on April 19, 2024

DMD Fast Forward. Published on November 8, 2012 as DOI: 10.1124/dmd.112.049460
This article has not been copyedited and formatted. The final version may differ from this version.

Figure Legends

Fig. 1 Simple PBPK models for ICZ (A), GEM/GEM-glu (B), and repaglinide (C). See Materials and Methods for abbreviations.

Fig. 2 Concentration profiles of ICZ (A), GEM and GEM-glu (B), and repaglinide (C) in blood.

(A) Based on the PBPK model (Fig. 1A) and differential equations (Eqs. 11, 12), the time course of the ICZ concentration in blood ($C_{b,icz}$) after 3 days of repeated administration (100 mg, p.o., b.i.d.) was reproduced using the PK parameters shown in Table 1. The solid line and the open circles indicate the simulated time course and the observed values (Jaakkola et al., 2005), respectively.

(B) Based on the PBPK model (Fig. 1B) and differential equations (Eqs. 16-21), the time courses of the GEM and GEM-glu concentration in blood ($C_{b,gem}$ and $C_{b,glu}$, respectively) after 3 days of repeated administration of GEM (600 mg, p.o., b.i.d.) were reproduced using the PK parameters shown in Table 1. The solid line and the open circles indicate the simulated time course and the observed values (Tornio et al., 2008), respectively, for GEM; the dotted line and the closed circles indicate the simulated time course and the observed values (Tornio et al., 2008), respectively, for GEM-glu.

Downloaded from dmd.aspetjournals.org at ASPET Journals on April 19, 2024

DMD Fast Forward. Published on November 8, 2012 as DOI: 10.1124/dmd.112.049460
This article has not been copyedited and formatted. The final version may differ from this version.

(C) Based on the PBPK model (Fig. 1C) and differential equations (Eqs. 22-26), the time courses of the repaglinide concentration in blood ($C_{b,s}$) for the 4 conditions (control, +ICZ, +GEM and +ICZ+GEM) were reproduced using the parameters shown in Table 2. The concentration profiles for ICZ and GEM/GEM-glu were simultaneously analyzed using Eqs. 11, 12 and 16-21, respectively, to provide the inhibitor concentrations. The solid line and open circles indicate the simulated time course and the observed values, respectively, for the control condition; the dotted line and open squares indicate the simulated time course and the observed values, respectively, for the +ICZ condition; the broken line and open triangles indicate the simulated time course and the observed values, respectively, for the +GEM condition; and the chain line and closed circles indicate the simulated time course and the observed values, respectively, for the +ICZ+GEM condition.

Fig. 3 Observed (A) and simulated (B) concentration profiles of repaglinide in an interaction study with GEM administered at different dosing intervals

(A) Reported repaglinide concentration profiles in healthy volunteers who received a single oral dose of repaglinide (0.25 mg) at different times after GEM (600 mg, p.o., b.i.d., for 3 days) (Backman et al., 2009). The solid line and open circles represent the

Downloaded from dmd.aspetjournals.org at ASPET Journals on April 19, 2024

DMD Fast Forward. Published on November 8, 2012 as DOI: 10.1124/dmd.112.049460
This article has not been copyedited and formatted. The final version may differ from this version.

profiles for the control condition (without GEM); the broken line and closed squares for the 1 hr interval condition; the chain line and closed triangles for the 24 hr interval condition; the double chain line and closed circles for the 48 hr interval condition; and the dotted line and asterisks for the 96 hr interval condition.

(B) Blood concentration profiles of GEM and repaglinide, assuming the same dosing regimen as in panel (A), were simulated based on the PBPK model shown in Figs. 1B and 1C together with the parameters estimated in the present study (Tables 2). The same line as in Fig. 3A was used for each condition.

Fig. 4 Sensitivity analysis of the paremeters obtained in this study

The concentration profiles of repaglinide were simulated using different values for fm_{2C8} (A and B), $K_{i,1B1,gem}$ (C and D), or $K_{i,3A4,icz}$ (E and F), with other parameters fixed at the same values as in Fig. 2C (the original values for fm_{2C8}, $K_{i,1B1,gem}$, and $K_{i,3A4,icz}$ were 0.801, 3,560 μg/L, and 0.0477 μg/L, respectively). The symbols and lines are same as in Fig. 2C.

Downloaded from dmd.aspetjournals.org at ASPET Journals on April 19, 2024

DMD Fast Forward. Published on November 8, 2012 as DOI: 10.1124/dmd.112.049460
This article has not been copyedited and formatted. The final version may differ from this version.

Table 1 PK parameters for inhibitors

Parameters	Units	Values	Sources
for ICZ			
Bioavailability		0.55	Thummel et al., 2011
CL_{tot} (plasma)	L/hr	21.4	Thummel et al., 2011
CL_{tot} (blood)	L/hr	36.9	CL_{tot} (plasma) / R_b
f_e		< 0.01	Thummel et al., 2011
CL_h (blood)	L/hr	36.9	assuming $CL_r = 0$
F_h		0.575	$1\text{-}CL_h/Q_h$
F_aF_g		0.957	Bioavailability / F_h
f_p		0.002	Thummel et al., 2011
R_b		0.58	Kato et al., 2008
cLogP		6.05	calculated by using ChemDraw Ultra 7.0
K_p		6.67	Eq. 14
f_h		0.000300	Eq. 13
Dose	μg	100,000	Niemi et al., 2003a
k_a	hr^{-1}	0.121 ± 0.037	*
V_b	L	59.2 ± 36.2	*

Downloaded from dmd.aspetjournals.org at ASPET Journals on April 19, 2024

DMD Fast Forward. Published on November 8, 2012 as DOI: 10.1124/dmd.112.049460
This article has not been copyedited and formatted. The final version may differ from this version.

CL_{int}	L/hr	14,700 ± 2,600	*
$C_{b,0}$	μg/L	98	Jaakkola et al., 2005
$C_{h,0}$	μg/L	1,131	assuming $C_{h,0} = C_{b,0} \times K_p / R_b$

for GEM

Bioavailability		0.98	Thummel et al., 2011
CL_{tot} (plasma)	L/hr	7.14	Thummel et al., 2011
CL_{tot} (blood)	L/hr	12.9	CL_{tot} (plasma) / R_b
f_e		< 0.01	Thummel et al., 2011
CL_h (blood)	L/hr	12.9	assuming $CL_r = 0$
F_h		0.85	$1\text{-}CL_h/Q_h$
F_aF_g		1	Bioavailability > F_h
f_p		0.0065	Shitara et al., 2004
f_b		0.012	f_p / R_b
R_b		0.55	Kilford et al., 2009
f_h		0.013	Eq. 13
Dose	μg	600,000	Niemi et al., 2003a
k_a	hr^{-1}	3.13 ± 0.36	*

Downloaded from dmd.aspetjournals.org at ASPET Journals on April 19, 2024

DMD Fast Forward. Published on November 8, 2012 as DOI: 10.1124/dmd.112.049460
This article has not been copyedited and formatted. The final version may differ from this version.

Lag	hr	0.25	estimated to fit the blood concentration profile of GEM
V_b	L	13.3 ± 8.6	*
CL_{int1}	L/hr	199 ± 506	*
CL_{int2}	L/hr	32.6	$CL_{int,gem1}$ / $CL_{int,gem2}$ = 6.1
PS_{inf}	L/hr	8,470	$CL_{int,all}$ × 10
PS_{eff}	L/hr	2,010 ± 5,110	*
for GEM-glu			
f_p		0.115	Shitara et al., 2004
f_b		0.209	f_p / R_b
R_b		0.55	assumed to be the same as GEM
f_h		0.206	Eq. 13
V_b	L	5.2	blood volume
CL_{NH}	L/hr	1.57	glomerular filtration rate × $f_{b,glu}$
$CL_{int,h}$	L/hr	12.5 ± 2.7	*
PS_{inf}	L/hr	469	assuming $f_b \cdot PS_{inf,gem} = f_b \cdot PS_{inf,glu}$
PS_{eff}	L/hr	100 ± 20	*

Downloaded from dmd.aspetjournals.org at ASPET Journals on April 19, 2024

DMD Fast Forward. Published on November 8, 2012 as DOI: 10.1124/dmd.112.049460
This article has not been copyedited and formatted. The final version may differ from this version.

*; optimized by fitting analysis. See Materials and Methods for abbreviations.

Downloaded from dmd.aspetjournals.org at ASPET Journals on April 19, 2024

DMD Fast Forward. Published on November 8, 2012 as DOI: 10.1124/dmd.112.049460
This article has not been copyedited and formatted. The final version may differ from this version.

Table 2 PK parameters for repaglinide and inhibition parameters

Parameters	Units	Values	Sources
Bioavailability		0.625	Hatorp, 2002
CL_{tot} (plasma)	L/hr	32.6	Hatorp, 2002
CL_{tot} (blood)	L/hr	52.6	CL_{tot} (plasma) / R_b
f_e		0.001	van Heiningen et al., 1999
CL_h (blood)	L/hr	52.6	assuming $CL_r = 0$
F_h		0.40	$1\text{-}CL_h/Q_h$
F_aF_g		1	Bioavailability > F_h
f_p		0.015	Hatorp, 2002
f_b		0.025	f_p / R_b
R_b		0.6	van Heiningen et al., 1999
Dose	μg	250	Niemi et al., 2003a
k_a	hr^{-1}	4.51 ± 1.87	*
Lag	hr	1.20 ± 0.06	*
V_b	L	8.38 ± 9.02	*
$f_h \cdot CL_{int}$	L/hr	5.63 ± 4.88	*
$f_b \cdot PS_{inf}$	L/hr	192 ± 127	*

Downloaded from dmd.aspetjournals.org at ASPET Journals on April 19, 2024

DMD Fast Forward. Published on November 8, 2012 as DOI: 10.1124/dmd.112.049460
This article has not been copyedited and formatted. The final version may differ from this version.

$f_h \cdot PS_{eff}$	L/hr	15.4	Yabe et al., 2011; Ménochet et al., 2012; Jones et al., 2012
k_{12}	hr^{-1}	2.62 ± 3.60	*
k_{21}	hr^{-1}	1.23 ± 0.30	*
fm_{2C8}		0.801 ± 0.049	*
$K_{i,3A4,icz}$	μg/L	0.0477 ± 0.0365	*
$K_{i,app,2C8}$	μM	20	Ogilvie et al., 2006
$k_{inact,2C8}$	hr^{-1}	12.6	Ogilvie et al., 2006
$k_{deg,2C8}$	hr^{-1}	0.03013	Yang et al., 2008
$K_{i,1B1,gem}$	μg/L	3,560 ± 2,530	*
$K_{i,1B1,glu}/K_{i,1B1,gem}$		0.385	Shitara et al., 2004; Nakagomi-Hagihara et al., 2007

*; optimized by fitting analysis. See Materials and Methods for abbreviations.

Downloaded from dmd.aspetjournals.org at ASPET Journals on April 19, 2024

DMD Fast Forward. Published on November 8, 2012 as DOI: 10.1124/dmd.112.049460
This article has not been copyedited and formatted. The final version may differ from this version.

Table 3 Repaglinide AUC increase produced by concomitant GEM administration at various timings/doses

	Fold change in repaglinide AUC produced by GEM	
Report 1 (Backman et al., 2009)		
Dosing interval between GEM and repaglinide	Simulated	Reported
1 hr	6.49	7.56
24 hr	1.78	2.86
48 hr	1.25	1.42
96 hr	1.05	0.98
Report 2 (Honkalammi et al., 2011)		
Dosing interval between GEM and repaglinide	Simulated	Reported
0 hr	4.85	4.98
1 hr	6.49	6.36
3 hr	5.22	6.59

Downloaded from dmd.aspetjournals.org at ASPET Journals on April 19, 2024

DMD Fast Forward. Published on November 8, 2012 as DOI: 10.1124/dmd.112.049460
This article has not been copyedited and formatted. The final version may differ from this version.

6 hr	3.93	5.43

Report 3 (Honkalammi et al., 2012)

Dose of GEM	Simulated	Reported
30 mg	3.35	3.40
100 mg	4.22	5.57
600 mg	6.49	7.04

See text for details.

Downloaded from dmd.aspetjournals.org at ASPET Journals on April 19, 2024

Figure 1

A
Gastrointestine
FxFg, ka
Qh
Blood
Cb, Vb, fb
Liver
Ch, Vh, fh
CLint
Qh
B
Gastrointestine
FxFg, kx, Lag
Qh
Blood
Cb, Vb, fb
Liver extracellular space
Ce, Ve, fe
Liver extracellular space (glu)
Ce, Ve, fe
Qh
Blood (glu)
Cb, Vb, fb
CLNH,glu
PSinf
PSeff
PSinf,glu
PSeff,glu
Liver
Ch, Vh, fh
Liver (glu)
Ch, Vh, fh
CLint2
CLint1
CLint,glu
C
Peripheral
Xsub
Gastrointestine
k21
k12
FxFg, kx, Lag
PSeff
Qh
Blood
Cb, Vb, fb
Liver extracellular space
Ce, Ve, fe
Liver
Ch, Vh, fh
CLint
Qh
PSinf

Figure 2

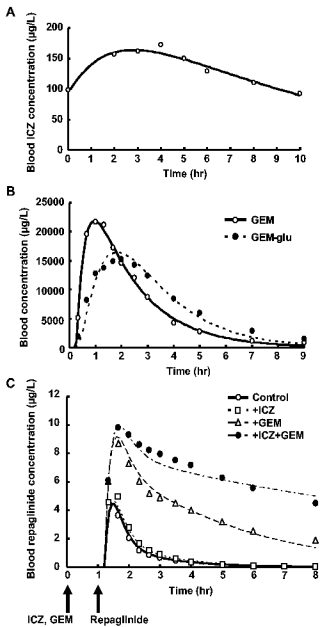
A
Blood ICZ concentration (μg/L)
200
150
100
50
0
0 1 2 3 4 5 6 7 8 9 10
Time (hr)
B
Blood concentration (μg/L)
25000
20000
15000
10000
5000
0
GEM
GEM-glu
0 1 2 3 4 5 6 7 8 9
Time (hr)
C
Blood repaglinide concentration (μg/L)
12
10
8
6
4
2
0
Control
+ICZ
+GEM
+ICZ+GEM
0 1 2 3 4 5 6 7 8
Time (hr)
ICZ, GEM
Repaglinide

Figure 3

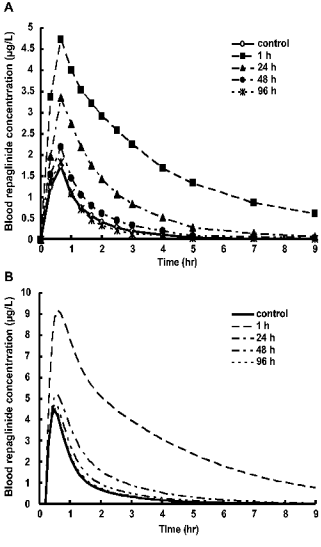
A
Blood repaglinide concentration (μg/L)
Time (hr)
control
1 h
24 h
48 h
96 h
B
Blood repaglinide concentration (μg/L)
Time (hr)
control
1 h
24 h
48 h
96 h

Figure 4

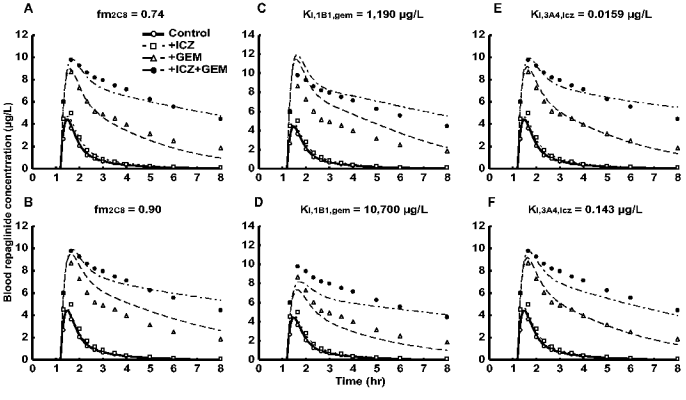
A
fm2C8 = 0.74
Control
- □ - +ICZ
- △ - +GEM
- ● - +ICZ+GEM
C
KI,1B1,gem = 1,190 μg/L
E
KI,3A4,Icz = 0.0159 μg/L
B
fm2C8 = 0.90
D
KI,1B1,gem = 10,700 μg/L
F
KI,3A4,Icz = 0.143 μg/L
Blood repaglinide concentration (μg/L)
Time (hr)